Supplemental Figure S1

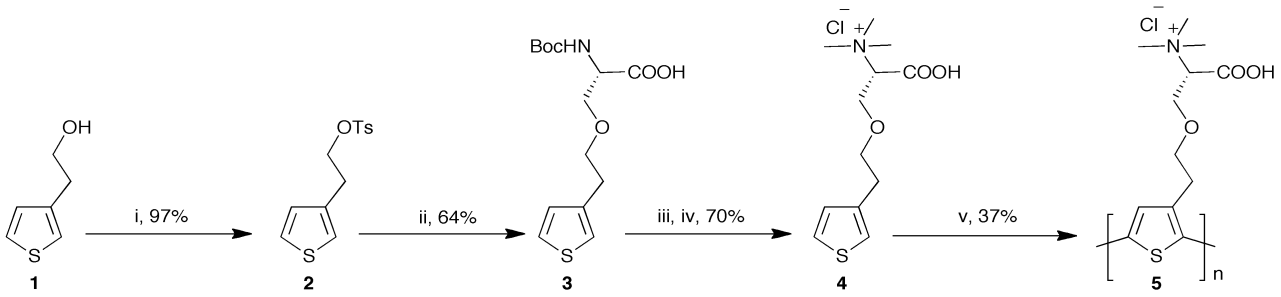

FIGURE S1. Reagents and conditions for the synthesis of PBAT. (1) 2-(Thiophene-3-yl) ethanol; (2) 2-(3-thienyl)-*p*-toluenesulfonyl ethanol; (3) (*S*)-3-[2-(3-thienyl)-ethoxy]-2-*tert*-butoxycarbonylamino-propionic acid; (4) (*R*)-1-carboxy-*N*,*N*,*N*-trimethyl-2-(2-(thiophen-3-yl)ethoxy)ethanaminium; (5) Poly- ((*R*)-1-carboxy-*N*,*N*,*N*-trimethyl-2-(2-(thiophen-3-yl)ethoxy)ethanaminium); (i) 1. Acetyl bromide, methanol; 2. NIS, chloroform/acetic acid (1:1); (ii) K_2CO_3, PEPPSI-IPr, toluene/methanol (1:1); (iii) 1. NaOH, H_2O, dioxane; 2. $FeCl_3$, TBA-triflate, chloroform. (iv) 1. p-TsCl, chloroform/pyridine (7:1); 2. N-t-Boc-Thr, K_2CO_3, DMF; (v) 1. TFA, chloroform; 2. $FeCl_3$, TBA-triflate, chloroform.

Supplemental Figure S2

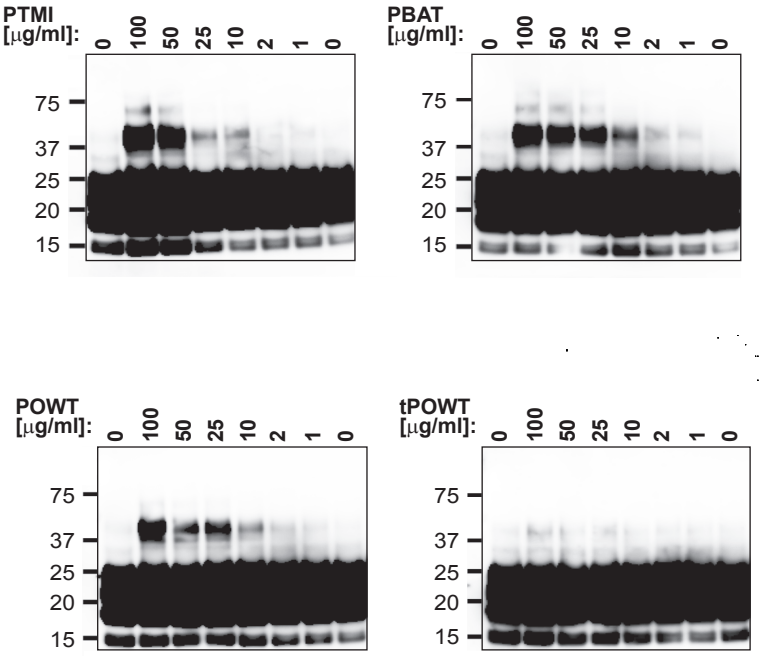

FIGURE S2. Longer exposures of selected immunoblots from Fig. 1B to evidence the appearance of higher-order aggregates in the samples treated with PTMI, PBAT and POWT and their absence in the samples treated with tPOWT.

Supplemental Figure S3

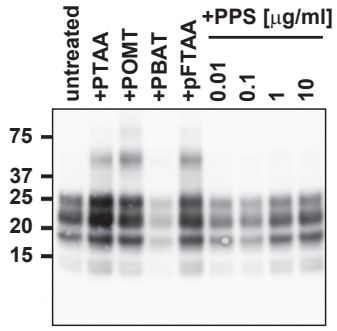

FIGURE S3. Comparison of the efficiency of the LCPs to PPS. Immunoblot of PK-digested RML6 samples after exposure to either 10 μg ml^{-1} PTAA, POMT, PBAT, pFTAA or increasing concentrations of PPS (0.01-10 μg ml^{-1}). Each sample contained 20 μg total protein. The untreated control in in lane 1 was supplemented with water. The anti-PrP antibody POM1 was used for detection. Molecular sizes are indicated in kilodaltons.

Supplemental Figure S4

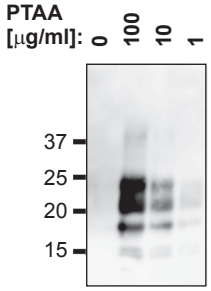

FIGURE S4. PTAA strongly protects PrP^{Sc} from PK digestion. Immunoblot of RML6 samples exposed to various concentrations of PTAA and subsequent digestion with an excess of PK at 2 mg ml^{-1} for 60 min. Each sample contained 45 μg of total protein. The anti-PrP antibody POM1 was used for the detection. Molecular sizes are indicated in kDa.

Supplemental Figure S5

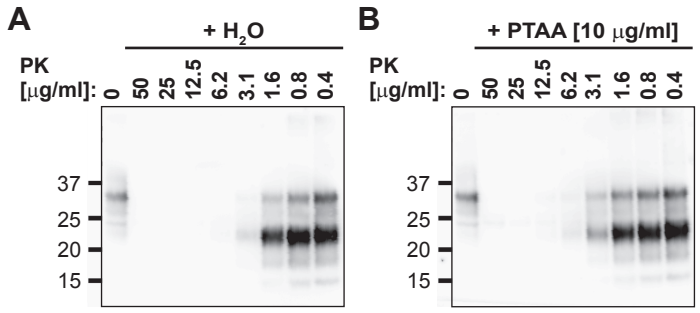

FIGURE S5. PTAA does not affect the sensitivity of PrP^C to PK digestion. (A) Samples of non-treated and (B) PTAA-treated non-infected CD1 brain homogenates were immunoblotted after limited PK digestion. Equal amounts of 20 μg protein from a CD1 brain homogenate were loaded on lanes 2-9. 2 μg of undigested protein from a CD1 brain homogenate was loaded as a control on Lane 1. The anti-PrP antibody POM1 was used for the detection. Molecular sizes are indicated in kDa.

Supplemental Figure S6

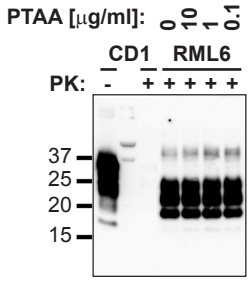

FIGURE S6. PTAA does not affect PK-digested PrP^{Sc}. All samples were digested with PK before exposure to PTAA and immunoblotting. Lane 1: 2 μg of total protein from an undigested CD1 brain homogenate. Lane 2: Marker. Lane 3: 10 μg of total protein from a PK digested CD1 brain homogenate. Lane 4: 10 μg of total protein from a RML6 brain homogenate digested before the addition of water. Lanes 5-7, 10 μg of total protein from a RML6 brain homogenate digested with 50 μg ml^{-1} PK before the addition of PTAA at various concentrations. The anti-PrP antibody POM1 was used for the detection. Molecular sizes are indicated in kDa.

Supplemental Figure S7

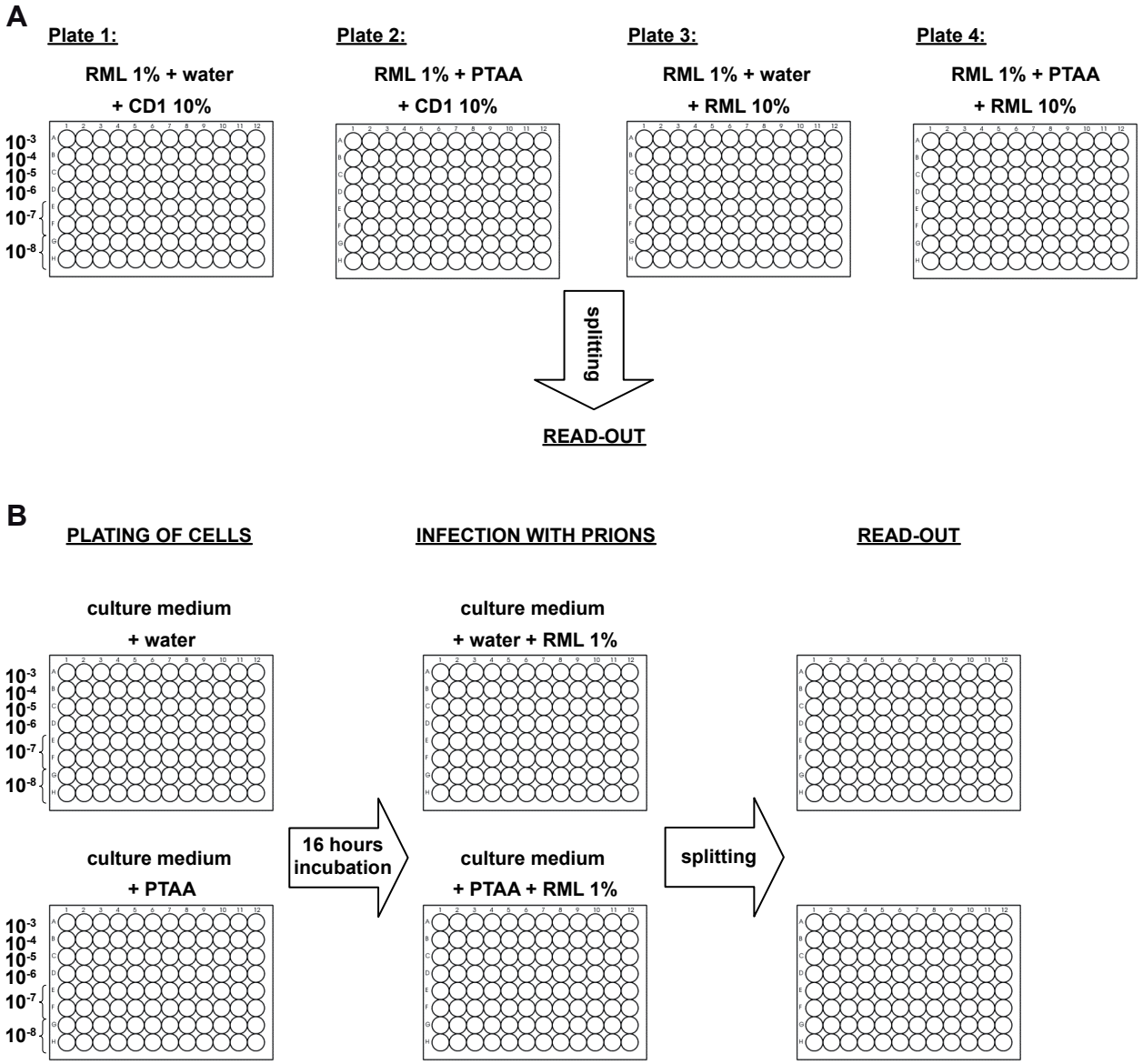

FIGURE S7. Experimental setup to verify the impact of PTAA on susceptibility of PK1-N2a cells to RML6. (A) Samples containing a 1% RML6 brain homogenate were treated with either water or PTAA prior to incubation with either a 10% non-infectious CD1 or a 10% RML6-infected brain homogenate. Infectivity of each sample was then determined in the SCEPA. (B) Cells were plated either in non-treated culture medium (upper) or in medium supplemented with PTAA (lower) 16 hours before infection with RML6. Infectivity of all samples was then determined in the SCEPA (statistical analysis in supplemental Tables S2 and S3).

Supplemental Figure S8

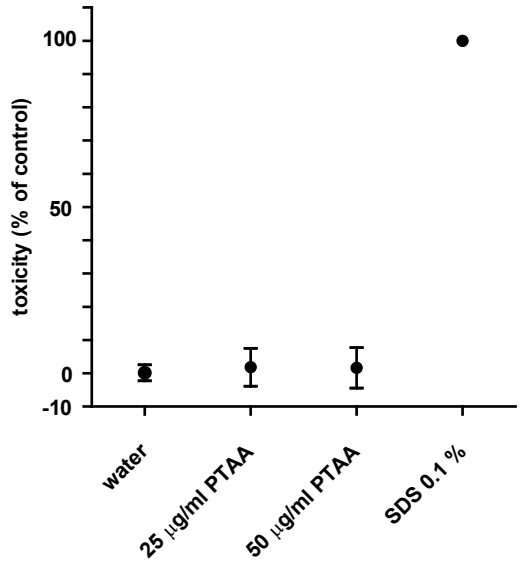

FIGURE S8. MTS cell viability assay upon treatment of PK1-N2a cells with PTAA at a concentration of 50 μg ml^{-1} and SDS as positive control. The optical density value measured for non-treated cells was taken as 100% viability. Each bar represents the mean cell viability ± SD of LCP-treated cells as a percentage of the values collected for non-treated cells. Measurements were performed in triplicates.

Supplemental Figure S9

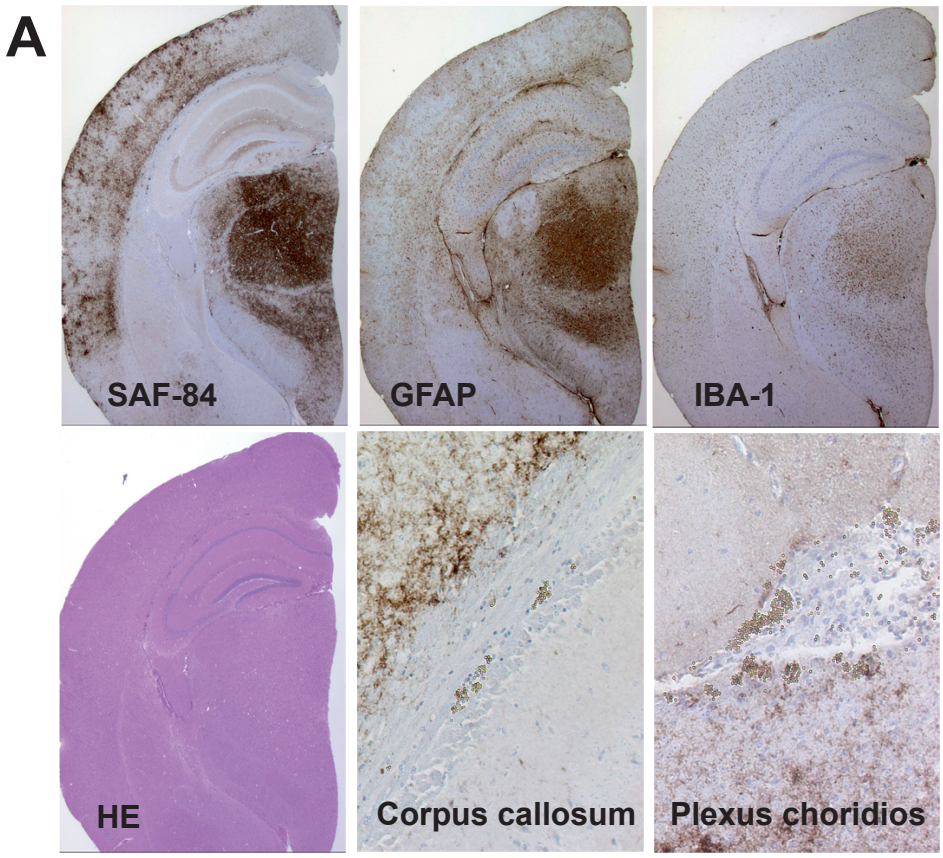

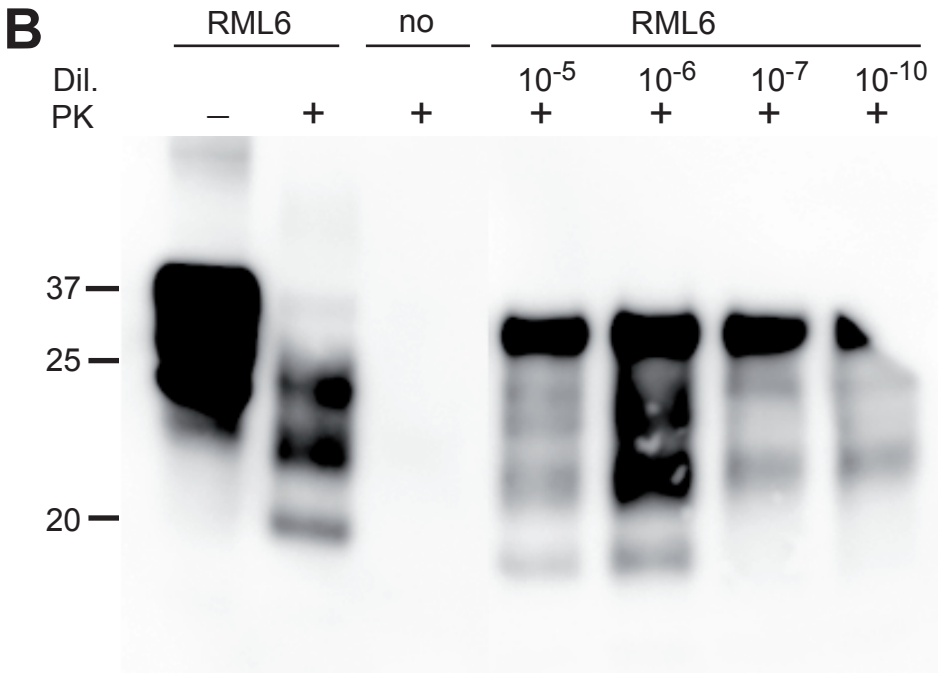

FIGURE S9. PSR1 beads efficiently capture and transmit prion infectivity. (A) Pathology of brain sections from tga20 mice. Mice inoculated with a 10^{-5} RML6 brain homogenate or with PSR1 beads incubated with RML6 show PrP^{Sc} depositions as visualized by the PrP antibody SAF84, astrocytic gliosis as evidenced by an antibody directed against GFAP and microglial activation as detected by the antibody IBA-1. Vacuoles are shown by hematoxylin and eosin staining (HE). Accumulation of beads was found in the Corpus callosum and Plexus choridios. (C) PK resistant material is present in tga20 mice inoculated with PSR1 incubated RML6 brain homogenate with different dilutions ranging from 10^{-5} to 10^{-10}. Control samples are labeled with no: brain homogenate from healthy mice and RML6: brain homogenate from mice inoculated with a 0.1% RML6. The molecular weight standard is shown in kilodaltons.

Supplemental Figure S10

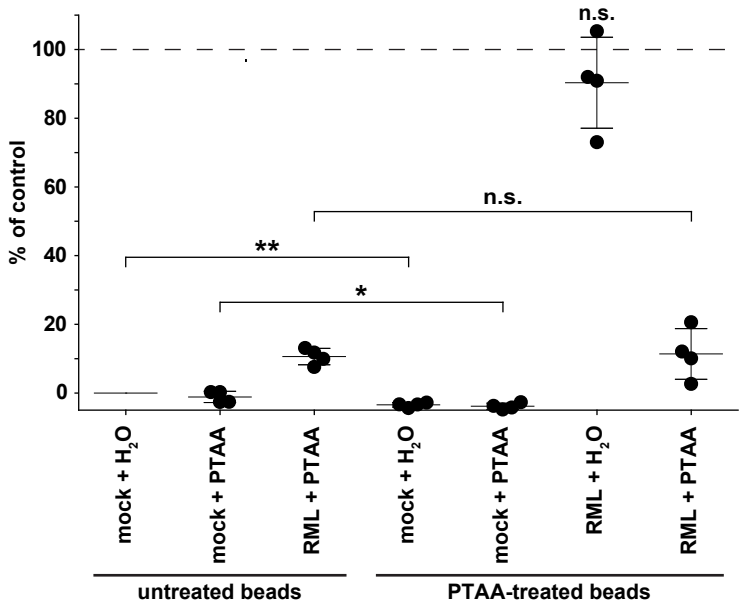

FIGURE S10. Control experiment for the MPA. Paramagnetic beads were either non-treated or treated with 100 μg/ml PTAA prior to capture of non-treated (+H_2O), PTAA-treated non-infected (mock: CD1 brain homogenate) or prion-infected (RML) samples. A significant reduction in the signal could be observed for the negative controls (CD1+H2O and CD1+PTAA). This statistical significance can be imputed to the small variability between technical replicas for the samples that yielded low fluorescence and therefore are to be considered as a statistical artifact (Supplemental Table S6).

Supplemental Figure S11

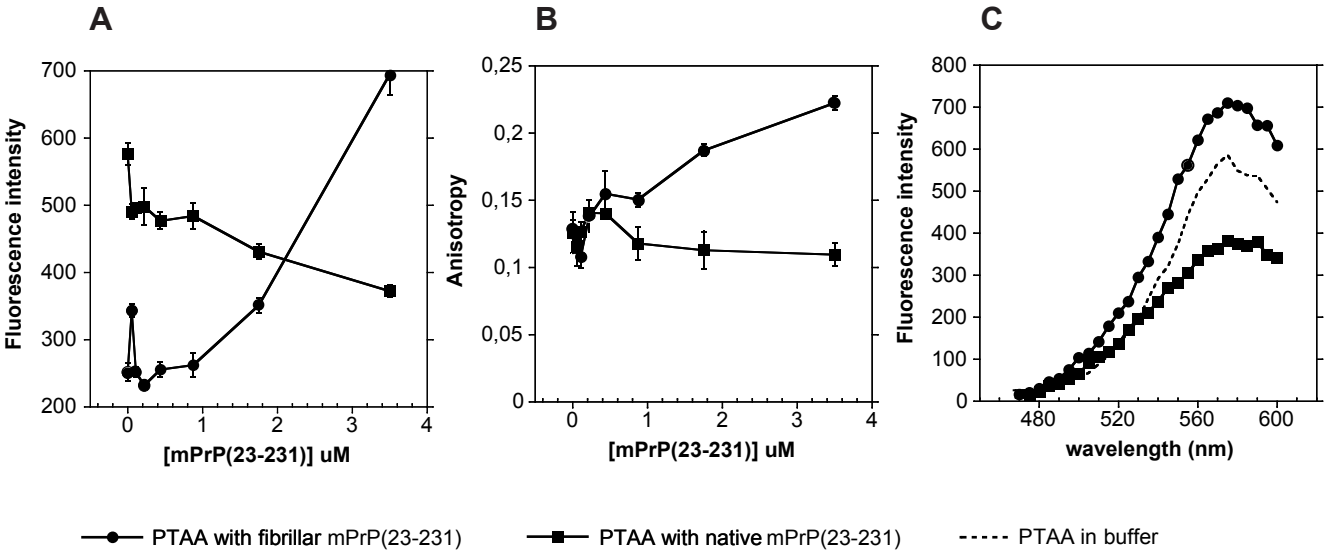

FIGURE S11. PTAA interacts with native $mPrP_{23-231}$. (A) Fluorescence intensity as a function of protein concentration reveals enhancement of fluorescence as $mPrP_{23-231}$ fibril concentration increases, whereas the fluorescence is quenched by elevated concentration of native $mPrP_{23-231}$. The average of triplicate experiment is presented. Error bars are the mean ± SD. (B) Fluorescence anisotropy demonstrates a two-mode binding process of PTAA to both native and fibrillar mPrP(23-231). The average of triplicate experiment is presented. Error bars are the mean ± SD. (C) Fluorescence maximum of PTAA in buffer is higher than for PTAA in presence of native $mPrP_{23-231}$ and lower than the fluorescence in presence of fibrillar $mPrP_{23-231}$. Representative spectra from triplicate experiment are presented. Measurements were performed with histagged $mPrP_{23-231}$ and fibrils.